Eur. Phys. J. B **33**, 109–114 (2003)
DOI: 10.1140/epjb/e2003-00147-x

THE EUROPEAN PHYSICAL JOURNAL B

Effect of interfacial alloying on the surface plasmon resonance of nanocrystalline Au-Ag multilayer thin films

R.K. Roy[1], S.K. Mandal[2], and A.K. Pal[1,a]

[1] Department of Materials Science, Indian Association for the Cultivation of Science, Calcutta-700 032, India
[2] Inter University Consortium for DAE Facilities, Sector-III, Block- LB/8, Bidhan Nagar, Calcutta-700 098, India

Received 17 October 2002 / Received in final form 26 February 2003
Published online 23 May 2003 –

Abstract. Nanocrystalline Au and Ag in multilayer thin film form with Au/Ag/Au structure were prepared by high pressure (∼40 Pa) d.c. sputtering techniques. The Ag concentrations in Ag_xAu_{1-x} films were changed from $x = 0$ to 1. These multilayer films with varying Ag concentration showed significant changes in microstructures obtained from TEM and XRD analyses. The optical absorption spectra of these multilayer films showed a single plasmon band confirming the formation of Au-Ag alloy. We ascribe this alloying to the interfacial reactions in nanophase limited at the Au-Ag interface. The red-shift and broadening of the plasmon bands with the increase in silver concentration could be associated to the increase in size of the nanoparticles and its distribution. The observed red shift in the plasmon band may be associated with the change in electronic structure at the Au-Ag interface due to configuration mixing of the atomic energy levels of Au and Ag.

PACS. 78.67.Pt Multilayers; superlattices – 78.66.Bz Metals and metallic alloys – 78.67.Bf Nanocrystals and nanoparticles

1 Introduction

Bimetallic nanostructures of gold and silver are found to be superior in some surface plasmon resonance (SPR) based devices to pure gold and silver, particularly in their use in chemical and biological sensors [1,2], catalytic activists [3,4] etc. The higher sensitivity of pure Ag in nanophase is a preferred choice in SPR based devices compared to other noble metals (Au, Cu etc.), but it is largely limited by its poor chemical stability. Protective layer of gold may not only improve its chemical stability, but also increase its detection sensitivity in SPR based devices. In fact, bimetallic nanostructures of Au-Ag either in alloy or multilayer form exhibit novel optical properties than that of pure gold or silver. Formation of Au-Ag alloys can lead to a single particle resonance and can be tuned between 400 nm (for pure Ag) and 520 nm (for pure Au), depending on the composition of the alloy. A flurry of experimental and theoretical activities over the past few decades [5–9] was devoted towards the understanding of the size and shape effects, broadening, effect of surrounding matrix etc. on the surface plasmon band of gold, silver and its nanocomposites. In contrast, studies on alloy nanoparticles are comparatively less [10–13]. A possible effect of alloying, not permissible in the bulk, could effect the formation of a sharp interface which would influence the microstructural and hence physical properties of the multilayer systems.

Most of the earlier works were concerned with either core-shell particles or $(Au_xAg_{1-x})_n$ clusters prepared by chemical routes. Link *et al.* [10], and more recently Chen *et al.* [11] studied the dependence of the surface plasmon absorption band on the composition of the alloy. They obtained a blue-shift of the plasmon resonance band with the increase Ag concentration. Recently, Gaudry *et al.* [12] reported the size and compositional effects of the bimetallic clusters on the optical absorption properties.

In contrast to others, we report here the formation of Au-Ag alloy prepared by sputtering technique in Au/Ag/Au multilayer thin film form. The influence of the Au-Ag interface, composition and size of the alloy nanoparticles on the optical properties are discussed.

2 Experimental

Multilayer thin films of nanocrystalline Au/Ag/Au structure (also denoted as Ag_xAu_{1-x}) were deposited onto fused silica substrate by sequential d.c. sputtering of Au and Ag targets (purity ∼99.995%) in argon plasma at a system pressure of ∼40 Pa. The concentration of the Ag in the whole structure assembly of Au/Ag/Au was varied from $x = 0.05$, 0.15, 0.5 and 0.75 by adjusting the time of deposition of silver while the durations of the

[a] e-mail: msakp@mahendra.iacs.res.in

top and bottom gold layers were kept constant. Besides these, two films containing nanocrystalline Au ($x = 0$) and Ag ($x = 1$) only were also deposited under identical deposition condition. The whole thickness of the layers Au/Ag/Au was varied around 10−20 nm. The substrates were placed on a heavy copper block that could be cooled by liquid nitrogen. The temperature of the substrates could be monitored and controlled by a copper-constantan thermocouple through an on/off electronic temperature controller. In the present case, we carried out all the deposition at a substrate temp $T_s \sim 273$ K. Before starting the actual deposition, the targets were pre-sputtered for 10 minutes with a shutter placed in between the target and the substrate. This shutter was also used to control the deposition time. All the depositions were performed at 1.5 kV and 50 mA with the target (2.5 cm diameter) and substrate distance of ∼2.5 cm. Films were simultaneously deposited under identical deposition conditions onto freshly cleaved NaCl (for TEM studies) and fused silica (for optical and XRD studies) substrates respectively. NaCl substrates had an initial carbon film to support the very thin nanocrystalline films for TEM observation. As the nature of fused silica and carbon film being amorphous, we presumed that the observation obtained from TEM studies would not prejudice the results reported here.

Optical absorbance spectra were recorded on a Hitachi U-3410 spectrophotometer and TEM images were obtained with a Hitachi H-600 transmission electron microscope.

Grazing incidence X-ray diffraction (GIXRD) of the multilayer as well as pure Au and Ag films were performed on a Rigaku Rotaflex RU-200 B X-ray diffractometer using CuK_α radiation ($\lambda = 1.54$ Å) with a grazing angle of incidence $\sim 8°$.

3 Results and discussion

For a physical mixture of Au and Ag nanoparticles, the optical absorbance should be dominated by two plasmon bands at ∼520 nm and 400 nm respectively. It is expected that with alloying, the individual identity of the Au and Ag nanoparticles would be lost and optical absorbance would show a single plasmon absorption band. The position of the plasmon peak in Ag_xAu_{1-x} alloy would depend mainly on the concentration of Ag, size of the nanoparticles (d) in the alloy and also be influenced by several other parameters [6]. The compositional dependence of the surface plasmon band in the Au-Ag alloy could be theoretically predicated by Mie theory [14]. In the quasistatic limit ($d \ll \lambda$) of dipole approximation, the optical absorption cross-section is given by:

$$\sigma_{ext}(\lambda) = 18\pi f \varepsilon_0^{3/2} \frac{\varepsilon_2(\omega)}{\lambda\left[(2\varepsilon_0 + \varepsilon_1(\omega))^2 + \varepsilon_2^2\right]} \qquad (1)$$

where $\varepsilon(\omega) = \varepsilon_1(\omega) + \varepsilon_2(\omega)$ and ε_0 are the dielectric constant of the metal particle and surrounding medium respectively and f is the concentration of metal particles.

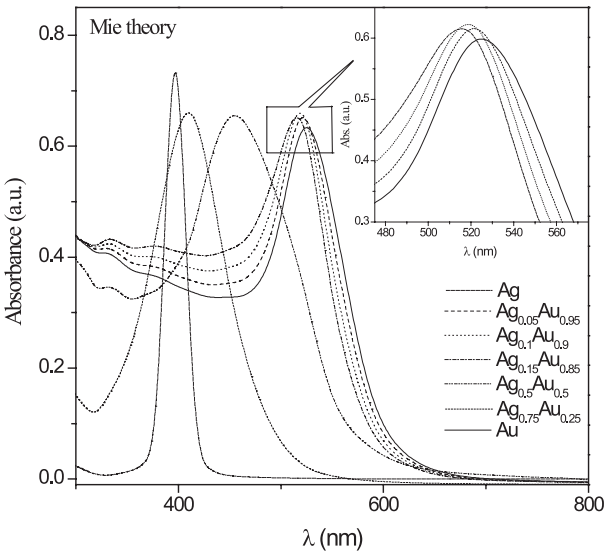

Fig. 1. Simulated optical absorbance spectra Ag_xAu_{1-x} films with $x = 0$ to 1 using Mie theory (Eq. (1)).

In case of Ag_xAu_{1-x} alloy, the dielectric constant could be assumed to vary with the composition-weighted average of the bulk Au and Ag dielectric constants [15] and is given by,

$$\varepsilon(x,\omega)|_{Ag_xAu_{1-x}} = x\varepsilon(\omega)|_{Ag} + (1-x)\varepsilon(\omega)|_{Au}. \qquad (2)$$

It is worthwhile to mention here that use of correct form of the dielectric function of alloy particles would result in an improved band shape to match the experimental spectra. Figure 1 shows the simulated absorbance spectra for Au-Ag alloy particles with the various Ag concentrations in accordance with the Mie equation (1). It clearly indicated a blue-shift of the resonance band from 520 nm ($x = 0$) to 400 nm ($x = 1$) with the increase in Ag concentration (x), as expected. For large Ag_xAu_{1-x} clusters, the plasmon band position ω_p would correspond to the following expression:

$$\omega_p|_{Ag_xAu_{1-x}} = x\omega_p|_{Ag} + (1-x)\omega_p|_{Au}. \qquad (3)$$

Figure 2 gives the variation of the plasmon peak position with x obtained from equations (1) and (3) respectively. While the equation (3) gives a linear dependence of the peak position with Ag concentration, peak position obtained from Mie theory deviated to some extent from linear variation. The experimental results obtained by various authors seemed reasonable with these predictions [10,11,16]. The experimental absorbance spectra obtained for Au/Ag/Au structure in this study is presented in Figure 3. The existence of single absorption maximum indicates the alloying of Ag nanoparticles with the Au nanoparticles. It further clearly indicates a red-shift of the plasmon band with the increase in Ag concentrations contrary to the equations (1) and (3) and also with the results obtained by other groups [10,11].

Before we discuss the discrepancy between the theoretical and our experimental results, we present below the microstructural information obtained from TEM and XRD

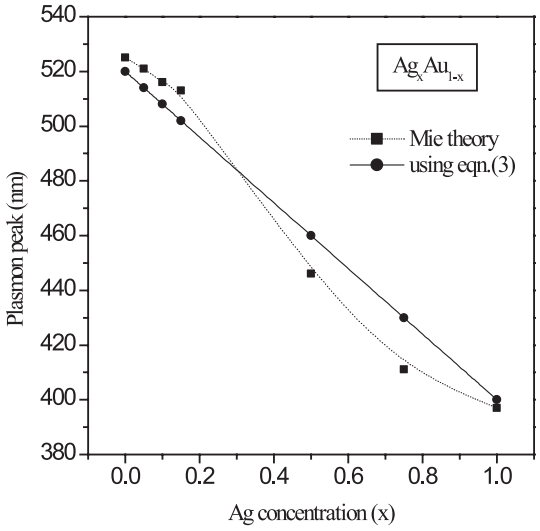

Fig. 2. Variation of plasmon peak with various Ag concentrations obtained from equations (1) and (3).

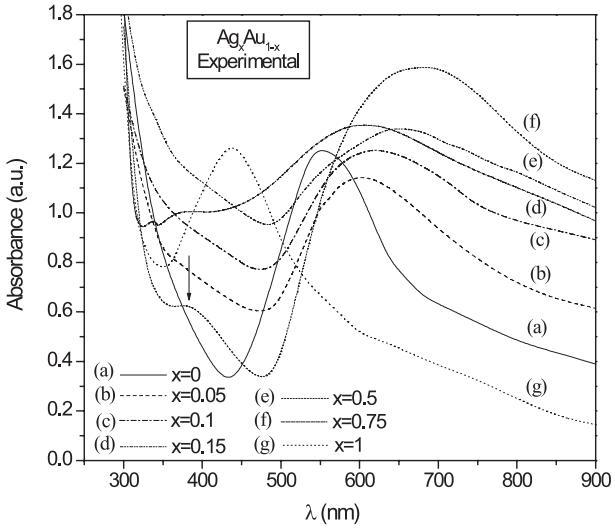

Fig. 3. Experimental optical absorption spectra of sputtered Au/Ag/Au multilayer thin films with varying Ag concentrations ($x = 0$ to 1).

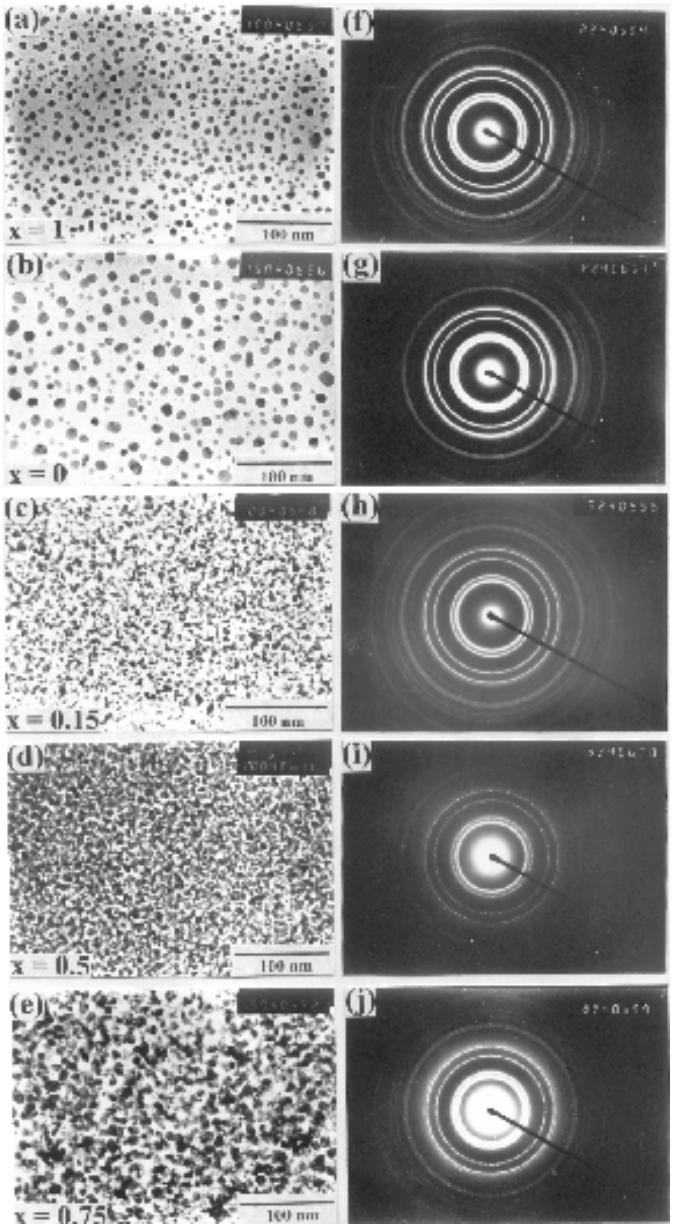

Fig. 4. TEM (a–e) and the corresponding electron diffraction patterns (f–j) of some representative films: (a) Au, (b) Ag, (c) Au:Ag = 85:15, (d) Au:Ag = 50:50 and (e) Au:Ag = 25:75.

analyses. Figure 4 presents the TEM image (4a–e) and corresponding electron diffraction patterns (4f–j) obtained for (a) Ag, (b) Au, (c) Au:Ag = 85:15, (d) Au:Ag = 50:50 and (e) Au:Ag = 25:75 nanoparticles respectively. Figures 4a and 4b clearly reveal well dispersed nanoparticles (having nearly spherical shape) with a very narrow size distribution for silver and gold films respectively. The average particle size obtained from Figures 4a and 4b for the Ag and Au nanoparticles was ∼3 nm and 4 nm respectively. Change in morphology with the deposition of multilayers is distinctly visible from Figures 4c–e for films with the ratio of Au:Ag = 85:15, Au:Ag = 50:50 and Au:Ag = 25:75 respectively. One can observe an increase in particle size and shape as well as its distribution in these multilayer films. These differed significantly from the microstructure of the pure Au and Ag metal films (Figs. 4a and b). Inhomogeneity in the distribution of nanocrystallites could also be appreciated. Formation of discontinuous and textured ring patterns (Fig. 4h–j) indicates the evolution of large oriented crystallites with the increase in Ag concentrations. Figure 5 shows the XRD profiles for Ag, Au, Ag_xAu_{1-x} ($x = 0.5$ and 0.75) films respectively. Both the Au (curve-a) and Ag nanoparticles exhibit (curve-d) similar cubic structure with the lattice parameter being almost same ($a = 4.0786$ Å for Au and 4.0862 Å for Ag). Both the spectra showed the peaks for reflections from (111), (200), (220) and (311) planes corresponding to the (fcc) cubic structure of Ag and Au. With the deposition of mulitilayers, one can observe a significant shift in the

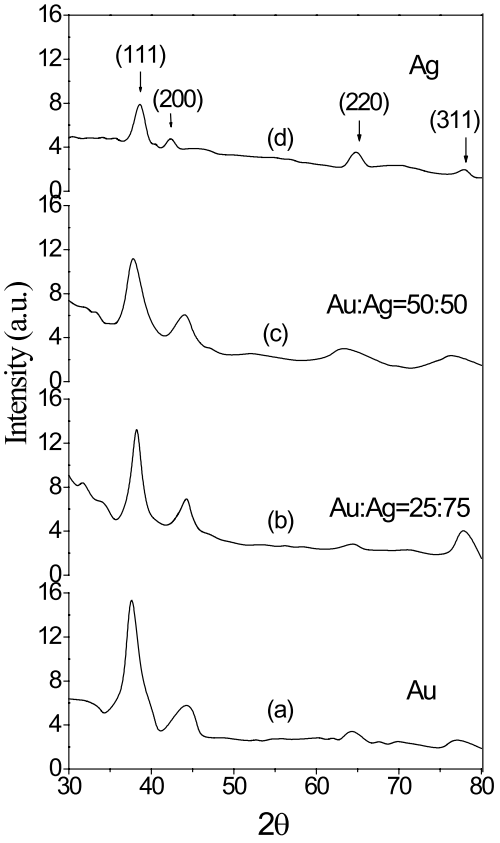

Fig. 5. XRD patterns of (a) Au, (b) Au:Ag = 25:75, (c) Au:Ag = 50:50 and (d) Ag nanocrystalline films.

peak positions and their line width (Fig. 5, curve-b and c) for all the films indicating the possible Au-Ag alloy formations. Similar trends are also reflected in the electron diffraction patterns shown in Figures 4e–h.

Now let us seek the root of possible mechanisms for alloy formation of the sputtered Au-Ag nanoparticles during its crystallization. In this case, as the argon gas pressure was kept quite high (∼40 Pa), the particles ejected from the target would undergo many collisions with the argon gas atoms and would subsequently nucleate by rapid condensation to form fine particles on the substrate. The kinetic energy of the sputtered atoms will be lowered during the collisions and as such would convey lesser thermal energy to the substrate. The substrate maintained at lower temperature (273 K) would act as a possible sink for the reduction in kinetic energy of the sputtered atoms impinging on it. So any diffusion or melting of the atoms could not be caused by this excess kinetic energy of atoms leading to alloy formation. The reason behind this alloying would be inherent to the nanoparticles themselves.

The alloying must have to take place either through the melting of individual Au and Ag atoms or by rapid dissolution of atoms in the solid phase. There are both theoretical and experimental evidences for the decrease of melting point of metals with the reduction in particle size [17,18]. Ercolessi *et al.* [18] showed a drastic reduction on the melting point of Au with decreasing cluster size by molecular dynamics simulation. The experimental evidence of a quasimolten state distinct from true thermodynamic molten state was provided by Ajayan *et al.* [19]. They demonstrated that a stable small particle on a substrate is trapped under a deep potential well and once out of these well can quasimelt between the various local minima states. Now, the melting points of both Au (1337 K) and Ag (1234 K) are quite higher than the substrate temperature maintained here during the deposition of Au/Ag/Au nanocrystalline multilayer films. Also the films did not encounter any further annealing at higher temperatures. So, alloying of the Au-Ag in the as-deposited films could not be achieved by the significant reduction in the melting points of Au and Ag nanocrystallites that must have to occur in its solid phase. This alloying was facilitated at higher concentration of silver nanocrystallites in the host Au nanocrystalline film. With the increase in the number density of silver nanocrystallites, the proximity of individual silver nanocrystals to Au nanocrystallites would decrease, favoring alloying of the nanocrystals. At very low concentration of silver nanoparticles in Au, this alloying will be very localized and the number density of Au_xAg_{1-x} nanocrystals in the host Au nanocrystals would be very small. Thus, one would observe a broad peak (not shown here in Fig. 3) located at the same peak position of the surface plasmon resonance of Au nanocrystallites.

The feasibility of rapid and spontaneous alloying of small metal clusters even in the solid phase was verified with theoretical and experimental evidence earlier [20–23]. It has been demonstrated that solute atoms can rapidly dissolute onto the host cluster at an anomalous rate even at room temperature, provided the cluster size is less than a critical size and with negative heat of solution [21]. In clusters of size greater than the critical size, rapid alloying remains confined with the surface and the core is still occupied by the host metal. The time scale of alloying is very fast and is less than 1−10 s. Such rapid and spontaneous alloy formation was observed with an *in situ* transmission electron microscopy for nanometer-sized Au-Cu system by Mori *et al.* [20], and more recently by Yasuda *et al.* for Au-Sn systems [22]. In our case the Ag layer (with varied concentration of Ag atoms in different films) is sandwiched between two Au layers. The impinging Ag atoms accumulating on the initial nucleation layer of Au rapidly relax and dissolute into the Au particles. Similar phenomena occur with the final layer of Au on the top of the Au/Ag/Au structure. So the alloying is essentially restricted into the interface between two Au layers. Although the real mechanism of such alloy formation is not well understood, formation of alloy at the interface in bimetallic system was observed by several workers [1,24,25] and our results are found to be consistent with them. The interfacial alloy formation is critically dependent on various parameters during the sputtering process *e.g.* thickness of the individual layers, sputtering rate, substrate temperature and ambient conditions etc.

The observation of alloy formation is confirmed by the appearance of a single resonance peak in the optical spectra as shown in Figure 3, and we ascribe the red-shift

in the plasmon peak with the increase in Ag fraction to the increase in particle size of the nanocrystallites at the Au-Ag interface. Also the distribution of the nanocrystallites at the interface is not very uniform and thereby leading to inhomogeneous broadening of the plasmon absorption bands. Similar red-shift in the plasmon bands was obtained for colloidal Au and Ag multilayer films by Musick *et al.* [26] and was attributed to the aggregation of nanoparticles. Gans *et al.* [27] earlier demonstrated the possibility of very large shift in the plasmon band towards the red if the particles retain ellipsoidal or irregular unisometric shapes. In fact, the Ag atoms dissolve in the solvent matrix Au with an enhanced solubility of the whole solution till the stoichiometric composition is attained (*i.e.* Au:Ag = 50:50). Further increase in Ag concentrations from the stoichiometry may lead to a fraction of simple physical mixture of Au and Ag atoms rather than complete alloying. In Figure 3 the optical absorption spectrum of the film with $x = 0.75$ in Ag_xAu_{1-x} shows an additional small peak around ∼400 nm (marked by arrow) and could be ascribed to the incomplete reactions of Ag atoms to the Au matrix. Also, the higher concentration of Ag atoms will lead to the formation of amorphous-like phase rather than any stable crystalline phase in Au-Ag interface. The broad rings in the diffractions with the increase in Ag concentrations reflect the evolution of amorphous-like phase (Figs. 4g–h). Such formation of amorphous-like phase in a very thin interface region (< 6 nm) in multilayer thin Au-In films obtained by ion-beam sputtering at 86 K was observed by Seyffert *et al.* [28]. By *in situ* electrical resistivity measurements of the Au-In multilayer films, they confirmed the existence of such an amorphous phase (a sharp drop in resistivity) and demonstrated that this interface amorphizations at low temperature did not arise out of any long-range thermal diffusion, but a phenomenon instigated by the interfacial reactions.

It appears that as we increase the Ag content, the dissolution of Ag in nano-Au may proceed surface alloying with the formation of homogeneous phase, intermixing of atoms in both layers occurs with the formation of metastable state and interfacial interaction between the two layers with no compound formation. Thus, the observed red shift upto a critical Ag content may arise basically due to surface alloying with the formation of a homogeneous phase. It was experimentally verified that upon dissolution of Ag into Au or *vice versa*, charge redistribution would follow. A charge compensation mechanism would then lead to a depletion of d electrons at the Au site accompanied by an increase in d electrons at the Ag site in the Au-Ag alloy. Au loses d electrons and gains s electrons while Ag loses s electrons and gains d electrons [25,29]. Photoemission and XANES results, as discussed by Bzowski *et al.* [29] and Tyson *et al.* [25] suggested that one would expect significant change in the Au and Ag d bands, core-level shift of Au $4f$ band away from the Fermi level and hybridization of the noble metal d bands modifying electronic structure with alloying. Narrowing of the alloy d band relative to d band of pure Au or Ag, a shift of the Au $4f$ core level and Ag $3d$ band to a higher binding energy and lower binding energy respectively were found to excellent indicators of the formation of Au-Ag alloy.

Thus, for the films containing a lower percentage of Ag, the excitation of the d electrons to the surface resonance state, as observed for individual Au and Ag crystals certainly got modified at the Au-Ag interface. We ascribe this modification to the interaction of the atomic energy levels of the Ag ($5s^14d^{10}$) and Au ($6s^14f^{14}5d^{10}$) at the Au-Ag interface. This configuration of the atomic levels mixing could be well speculated due to the non-spherical nature of the crystals at the disordered interface as clearly revealed by TEM images. Depending on the composition in the Au-Ag alloy, a rehybridization of the atomic levels would give rise to a different position of the SPR band in contrast to the Mie theory and other simplistic theoretical predictions for bulk alloying. In the Ag_xAu_{1-x} alloy, for a dilute concentration of the Ag layer ($x < 0.5$), the movement of Au $5d$ band (with respect to the Fermi level), which is most sensitive to chemical changes would play the crucial role in determining the SPR band positions. Beyond the stoichiometric compositions *i.e.* for $x > 0.5$, the rehybridization of the atomic levels would tend to break and a simple admixture of the components dominated by interfacial interaction rather than alloying would be dominant. Consequently, the SPR band would show features of the individual elements of the alloy, as observed experimentally.

4 Conclusion

The optical absorption properties of Au/Ag/Au films prepared by high pressure sputtering were studied. The films showed a single resonance peak in the optical absorption characteristics and could be attributed to the typical plasmon band corresponding to the Au-Ag alloying at the Au-Ag interface in nanocrystalline phase. The plasmon band showed red-shift with the increase in Ag concentrations and was attributed to the change in the particle size, shape and its distribution. This would possibly result in a configuration mixing of the atomic energy levels at the Au-Ag interface. Increase in Ag concentration ($x > 0.5$) far from stoichiometry led to incomplete interfacial reactions and possibly an amorphous-like phase. This further led to an appearance of a weak plasmon band at ∼400 nm indicating the physical mixture of a fraction of Ag and Au nanoparticles.

One of us, R.K.R. wishes to thank the Council of Scientific and Industrial Research, Government of India, for granting him a fellowship for executing this work.

References

1. T.T. Ehler, L.J. Noe, Langmuir **11**, 4177 (1995)
2. S.A. Zynio, A.V. Samoylov, E.R. Surovtseva, V.M. Mirsky, Y.M. Shirshov, Sensors **2**, 62 (2002)

3. P. Mulvaney, M. Giersig, A. Henglein, J. Phys. Chem. **97**, 7061 (1993)
4. J. Schwank, Gold Bull. **16**, 98 (1983)
5. U. Kreibig, M. Vollmer, *Optical Properties of Metal Clusters* (Springer, Berlin, 1995)
6. U. Kreibig, L. Genzel, Surf. Sci. **156**, 678 (1985)
7. W.A. De Heer, Rev. Mod. Phys. **65**, 611 (1993)
8. S.K. Mandal, R.K. Roy, A.K. Pal, J. Phys. D **35**, 2198 (2002); S.K. Mandal, R.K. Roy, A.K. Pal, J. Phys. D **36**, 261 (2003)
9. J.H. Hodak, A. Henglein, G.V. Hartand, J. Chem. Phys. **112**, 5942 (2000)
10. S. Link, Z.L. Wang, M.A. El-Sayed, J. Phys. Chem. B **103**, 3529 (1999)
11. Dong-Hwang Chen, Cheng-Jia Chen, J. Mater. Chem. **12**, 1557 (2002)
12. M. Gaudry, J. Lerme, E. Cottancin, M. Pellarin, J.-L. Vialle, M. Broyer, B Prével, M. Treilleux, P. Mélinon, Phys. Rev. B **64**, 085407 (2001)
13. G.L. Hornyak, C.J. Patrissi, E.B. Oberhauser, C.R. Martin, J.-C. Valmalette, L. Lemarie, J. Dutta, H. Hofmann, NanoStructured Materials **9**, 571 (1997)
14. G. Mie, Ann. Physik **25**, 377 (1908)
15. P.B. Jhonson, R.W. Christy, Phys. Rev. B **6**, 4370 (1972).
16. R.G. Freeman, M.B. Hommer, K.C. Grabar, M.A. Jackson, M.J. Natan, J. Phys. Chem. B **100**, 718 (1996)
17. J.P. Borel, Surf. Sci. **106**, 1 (1981)
18. F. Ercolessi, W. Andreoni, E. Tosatti, Phys. Rev. Lett. **66**, 911 (1991)
19. P.M. Ajayan, L.D. Marks, Phys. Rev. Lett. **63**, 279 (1989)
20. H. Yasuda, H. Mori, M. Komatsu, K. Takeda, H. Fujita, J. Electron Microsc. **41**, 262 (1992)
21. H. Yasuda, H. Mori, Phys. Rev. Lett. **69**, 3747 (1992)
22. H. Yasuda, K. Furuya, Eur. Phys. J. D **10**, 279 (2000)
23. Y. Shimizu, S. Sawada, K.S. Ikeda, Eur. Phys. J. D **4**, 365 (1998)
24. R.E. Watson, J. Hudis, M.L. Perlman, Phys. Rev. B **4**, 4139 (1971)
25. C.C. Tyson, A. Bzowski, P. Kristof, M. Kuhn, R. Sammynaiken, T.K. Sham, Phys. Rev. B **45**, 8924 (1992)
26. M.D. Musick, C.D. Keating, L.A. Lyon, S.L. Botsko, D.J. Pena, W.D. Holliway, T.M. McEvoy, J.N. Richardson, M.J. Natan, Chem. Mater. **12**, 2869 (2000)
27. R. Gans, Ann. Physik **37**, 881 (1912)
28. M. Seyffert, A. Siber, P. Ziemann, Phys. Rev. Lett. **67**, 3792 (1991)
29. A. Bzowski, T.K. Sham, R.E. Watson, M. Weinert, Phys. Rev. B **51**, 9979 (1995)